

Electronic Supporting information (ESI) for

**Tailor-made graphite oxide-DAB poly(propylene imine)
dendrimer intercalated hybrids and their potential for
efficient CO₂ adsorption**

T. Tsoufis,^{a*} F. Katsaros,^a Z. Sideratou,^a G. Romanos,^a O. Ivashenko,^b P. Rudolf,^b
B.J. Kooi,^{b,c} S. Papageorgiou,^a and M.A. Karakassides^d

^a NCSR “Demokritos”, Institute of Advanced Materials, Physico-chemical Processes, Nanotechnology & Microsystems, GR15310, Athens, Greece.

^b Zernike Institute for Advanced Materials, University of Groningen, Nijenborgh 4, NL9747AG Groningen, The Netherlands.

^c Materials innovation institute M2i, University of Groningen, Nijenborgh 4, NL9747AG Groningen, The Netherlands.

^d Department of Materials Science and Engineering, University of Ioannina, GR45110 Ioannina, Greece.

CONTENTS

• Experimental section	2
• Instrumentation and analysis methods	2
• PXRD diffraction patterns (Figures S1, S2)	5
• XPS spectroscopy (Figure S3)	5
• FTIR spectroscopy (Figure S4)	6
• Raman measurements (Figure S5)	7
• TEM measurements (Figure S6)	7
• SEM measurements (Figure S7)	8
• CO₂ adsorption studies (Tables S1, S2, Figures S8, S9)	8
• TGA measurements Elemental Analysis (Figure S10, Table S3)	11
• References	12

* Corresponding author, e-mail: t.tsoufis@chem.demokritos.gr

Experimental Section

Materials: The various employed amine-terminated diaminobutane DAB₄, DAB₈, DAB₁₆ (G1, G2, G3 generation respectively) dendrimers exhibiting molecular weight of 300, 741, 1.622 Da correspondingly, were purchased by DSM Fine Chemicals.

Synthesis of Graphite Oxide: Aqueous dispersions of GO were produced starting from graphite powder using the well-established and widely recognized modified Staudenmaier's method.¹ In a typical procedure, 10 g of powdered graphite (purum, powder ≤0.2 mm; Fluka) were added to a mixture of concentrated sulfuric acid (400 ml, 95–97 wt%) and nitric acid (200 mL, 65 wt%) while cooling it in an ice-water bath. Potassium chlorate powder (200 g, purum, >98.0%; Fluka) was added to the mixture in small portions under stirring and cooling. The reaction was quenched after 18 h by transferring the mixture into distilled water. The oxidation product was finally washed with distilled water until constant pH value (pH=6) and dried at room temperature.

Synthesis of DAB intercalated Graphite Oxide: In a typical intercalation experiment, a sample of 50 mg of GO was dispersed in distilled water using a combination of sonication and prolonged stirring at ambient conditions. Next, the pH of the resulting GO colloidal suspension was tuned at 9 by adding a few drops of dilute (0.5 N) aqueous solution of NaOH. Subsequently, an aqueous solution containing an excess quantity (150 mg, 3x times) of the selected DAB dendrimer (DAB₄, or DAB₈, or DAB₁₆) was added drop-wise. Each GO-DAB mixture was allowed to further stir for 48 h at 45°C before isolation of the resulting GO-DAB solids by centrifugation at 9.000 rpm, followed by thorough washing with water in order to remove the excess, unreacted DAB, until the pH of supernatant reached the value of 7. Finally, the synthesized materials were received after lyophilization, yielding the final hybrids: GO-DAB₄, GO-DAB₈, GO-DAB₁₆, and GO-DAB₆₄. In order to study the effect of different DAB loadings into GO, we choose as model system the GO-DAB₈ sample (1:3 weight ratio). In a similar synthetic approach to that described above, samples of 50 mg of GO powder were dispersed into water with the aid of prolonged stirring and sonication, followed by tuning of the pH at 9 and drop-wise addition of aqueous solutions of DAB₈ in suitable portions to achieve the targeted GO-DAB₈ weight ratio (1:0.5, 1:3 and 1:10). Each mixture was then allowed to further stir for additional 48 h at room temperature before isolation of the resulting GO-DAB solids by centrifuging cycles at 9.000 rpm, followed by thorough washing with water until the pH of supernatant reached the value of 7 and finally dried at room temperature.

Reactions of alkylamines (*n*-butylamine, dodecylamine) with GO and intercalated GO-DAB₈ (1:3 weight ratio): The intercalation reactions of alkylamines into GO and/or GO-DAB₈ were performed according to previous, well established methodologies.^{1,2,3} In particular, the intercalation reaction of *n*-butylamine into GO-DAB₈ was conducted adopting a similar approach to that employed for the intercalation of DAB₈ into pristine GO. In detail, an excess quantity (90 mg) of *n*-butylamine was added into 20 ml of a 50%-50% water-ethanol solution. The derived solution of was slowly added into 30 ml of GO-DAB₈ solution (30 mg in 50% water-50% ethanol), and the mixture was left to react under stirring for 48 h in a slightly basic pH environment. The product of the reaction was collected by centrifugation at 9.000 washed thoroughly with water until the pH of supernatant reached the value of 7 and finally dried at room temperature.

Instrumentation and analysis methods

Powder X-ray powder diffraction data were collected on a D8 Advance Bruker diffractometer by using Cu K α radiation (40 kV, 40 mA) and a secondary-beam graphite monochromator. The patterns were recorded in a 2 θ range from 2 to 30°, in steps of 0.02° and counting time 2 s per step.

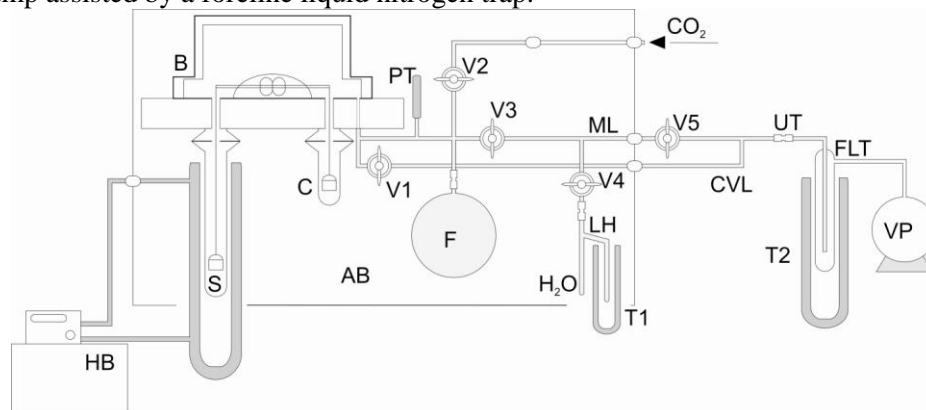
For the X-ray photoelectron measurements, the samples were dispersed in water and after very short sonication a small droplet of the suspension was drop-casted onto a gold substrate and left to dry at room temperature. The samples were then introduced in an ultra-high vacuum system via a loadlock and where they were kept under high vacuum for at least 12 hours before measurement, allowing the removal of volatile substances and/or solvents. X-ray photoelectron spectroscopy data were collected using an SSX-100 (Surface Science Instruments) spectrometer equipped with a monochromatic Al K α X-ray source (hv=1486.6 eV). The photoelectron take-off angle was 37° with respect to the surface normal and the energy resolution was set to 1.2 eV to minimize data acquisition time. All binding energies were referenced to the C 1s core level

line of the C-C bond at 285.0 eV and are given ± 0.1 eV. Spectral analysis included a Shirley background subtraction and peak fitting using mixed Gaussian-Lorentzian functions in a least-squares curve-fitting program (Winspec) developed at the LISE laboratory of the University of Namur, Belgium. The procedure consisted in fitting a minimum number of peaks that can reproduce the raw data and are consistent with the experimental resolution and the molecular structure of each analyzed sample. The substrates were freshly evaporated gold films supported on mica; four points were measured on each sample in order to guarantee the reproducibility of the results. For simplifying the comparison of the various presented XPS spectra, all intensities of C 1s core-level peaks were normalized to the corresponding peak of GO. The photoelectron peak intensities of each element, used to estimate the amount of each species on the surface, were normalized by the sensitivity factors of each corresponding element tabulated for the spectrometer used. The stability of all analyzed samples against damage induced by the X-ray beam and by secondary electrons produced by photoemission in the underlying substrate was verified by monitoring the lineshape and relative intensity of the C 1s, N 1s, and O 1s core-levels as a function of irradiation time. No evidence of structural degradation was observed even when irradiation was continued twice as long as the acquisition time used for the reported spectra. Raman spectra were recorded with a micro-Raman system RM 1000 Renishaw using a laser excitation line at 532 nm (Nd-YAG) in the range of 400–2.000 cm^{-1} . A power of 1 mW was used with 1 μm focus spot to avoid photodecomposition of the samples.

Scanning Electron Microscopy (SEM) images were recorded using a Jeol JSM 7401F Field Emission Scanning Electron Microscope equipped with Gentle Beam mode. Gentle Beam technology can reduce charging and improve resolution, signal-to-noise, and beam brightness, especially at low beam voltages (down to 0.1 kV). Transmission electron micrographs were obtained using a Technai T20 microscope (operating at 200 kV for both TEM and STEM modes). For the preparation of TEM samples a drop of the corresponding dispersion in hexane was deposited onto a holey-carbon grid and left to evaporate.

FT-IR studies were performed using a Nicolet 6700 Fourier Transformed Infrared spectrometer equipped with an Attenuated Total Reflectance accessory (ATR) with a diamond crystal (Smart Orbit™, Thermo Electron Corporation). The samples were molded into pellets using KBr (0.2 mg of sample and 200 mg of KBr). These pellets were firmly pressed against the diamond and spectra were recorded at 4 cm^{-1} resolution. A minimum number of 128 scans were collected and the recorded signal was averaged. Thermogravimetric analyses (TGA) were performed on a Setaram SETSYS Evolution 17 instrument using a heating rate of 5 $^{\circ}\text{C}/\text{min}$ under oxygen atmosphere. Elemental analysis was acquired by a Perkin Elmer 240 CHN elemental analyzer.

The CO_2 adsorption capacities of pristine GO (reference sample) and of the intercalated GO samples were obtained with the gravimetric technique. A schematic diagram of the apparatus applied for the performance of the experiments is showed in Scheme S1. The measurement system (B) (CI MK2-M5 recording microbalance - CI PRECISION) is a force restoration, full beam, electronic microbalance with high capacity of 5 g load, 0.1 μg readability and wide dynamic range (± 1 g) that can operate from high vacuum up to 150 kPa. The head (B) consists of a microbalance movement mounted on a rigid aluminium block which incorporates two hang-down ports and a vacuum/gas port. To conduct the CO_2 adsorption experiments, small amounts of GO and intercalated GO, (75 and 25 mg respectively) were introduced in the weighing pan of the balance. Both samples were outgassed at 80 $^{\circ}\text{C}$ under high vacuum (10^{-4} mbar) conditions, generated via a mechanical pump assisted by a foreline liquid nitrogen trap.



Scheme S1: The gravimetric set-up employed for CO_2 adsorption experiments of dry and wet GO and GO-DAB_8 samples.

Experiments were performed at 298 and 310 K. The CO₂ absorption/desorption isotherm was initially determined on the dry samples at several small pressure steps from 0 to 1000 mbar followed by outgassing of the sample (353.15 K, 10⁻⁴ mbar). Then the sample was left to equilibrate at a specific water vapour relative pressure. After mass relaxation (absorption equilibration) and without removing the water vapour from the measuring system, the sample was exposed sequentially at 5 different pressures of CO₂ from 200 to 1.000 mbars. The sample was regenerated again and left to equilibrate at the next water vapour relative pressure. In this way, three CO₂ absorption isotherms at 310.15 K were determined after having exposed the sample to three different relative pressures of water vapour (P/P₀= 0.03, 0.13, 0.35). For the dry GO sample, mass relaxation at each CO₂ pressure step was achieved after a period of 18 hours, while for the intercalated GO the required period was much more prolonged (48 hours). Water absorption was faster and the mass relaxation time depended on the water vapour pressure. The movement is of a double-sided construction, one side carrying the sample weight (S) and the other carrying counterbalance weight (C). Both the sample and the counterweight were suspended from two rigid lattice arms, which allow uniform expansion at elevated temperatures. To minimise buoyancy effects, the construction materials of the hanging rods, the pan carriers, the weighing pans and the counterweight were appropriately selected for achieving almost identical bulk volumes of the several accessories hung in the sample and counterweight compartments. Furthermore, a stainless steel manifold with diaphragm valves was constructed and attached to the vacuum/gas port of the balance. The coarse vacuum line of the manifold (CVL) was used for outgassing the solid sample after being placed into the weighing pan, whereas the upper manifold line (ML) was used for the introduction of CO₂ and H₂O vapour into the balance and for degassing water by successive melting/freezing cycles while vacuum pumping non-condensable gases through valve V4. During water degassing valve V3 was kept closed in order to avoid contamination of the measurement section of the manifold with water vapour. The pressure is measured with an absolute pressure electronic transducer (PT), (WIKA 0-1000mbar, and accuracy 0.02% full scale). The sample compartment was maintained at constant temperature to within ±0.01 K via a double walled glass vessel, with the thermal fluid (silicone oil) circulated by a JULABO (model MW12) constant temperature refrigerated/heating circulator (HP). A high volume (2.5 L) borosilicate glass flask (F) was attached to the upper manifold line through valve V2 in order to avoid drop of the pressure due to gas absorption by the samples. The balance head and measuring section of the manifold, enclosed between valves V1, V2, V4 and V5, were kept at ±0.1 K via an air bath, the temperature of which was controlled via an air-fan/resistance system and PID controller. Connection of the several glass components, e.g. the high volume flask (F), the H₂O-vessel (LH) and the foreline liquid nitrogen trap (FLT) of the mechanical vacuum pump (VP), with the metal tubes was achieved by SS-316 Ultra-Torr (UT) connectors (Cajon®). The valves of the system were SS-316 diaphragm valves equipped with compressed air actuators. The valve control and the readings of the balance, the temperature and pressure were implemented via a home-made virtual instrument application, developed in LabView® environment.

In the gravimetric analysis there is one major issue of concern in order to assess correctly the adsorption capacity and diffusivity of CO₂ in the dry and wetted GO and intercalated GO samples. This is to apply the most accurate correction for the buoyant forces introduced due to gas pressure and temperature changes. In the current work the static instead of the dynamic mode of operation was selected for performing the analysis and thereby other sources of error such as aerodynamic drag forces created by the flow of gases are negligible. Changes in the balance sensitivity due to changes in temperature can be also neglected since the balance head (electronics part) was maintained at ±0.1 K. The equation applied for the definition of the corrected mass uptake obtained from the microbalance was as follows:

$$m_{cor} = m_{dis} - m_{dis, init} + \Delta m \quad \text{with}$$

$$\Delta m = \frac{m_s}{\rho_s(T_s, P)} \rho_g(T_s, P) + \frac{m_1}{\rho_1} \rho_g(T_c, P) + \sum_{i=1} \frac{m_i}{\rho_i} \rho_g(T_s, P) - \sum_{j=1} \frac{m_j}{\rho_j} \rho_g(T_c, P) \quad (1)$$

where m_{cor} the corrected mass uptake, m_{dis} the display of the balance during gas uptake, $m_{dis, init}$ the initial display of the balance after outgassing, Δm the correction for buoyancy at each pressure (P), m_s/ρ_s the volume of the sample at the several pressures (P) up to 1 bar and temperature T_s , m_1/ρ_1 the volume (stable) of the component of the weighing section at the temperature of the air bath T_c , m_i/ρ_i the volume (stable) of the several components of the weighing section at the temperature of the sample T_s , m_j/ρ_j the volume (stable) of the several components of the counterweight section at the temperature of the air bath T_c , and $\rho_g(T, P)$ the density of the gas phase at a specific temperature and several pressures.

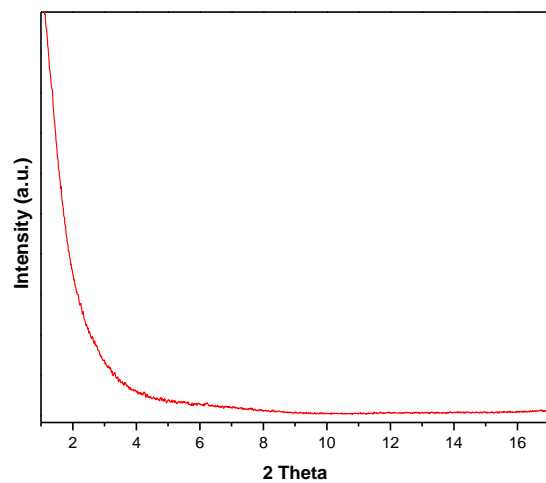


Figure S1. PXRD pattern of the GO-DAB₆₄ sample.

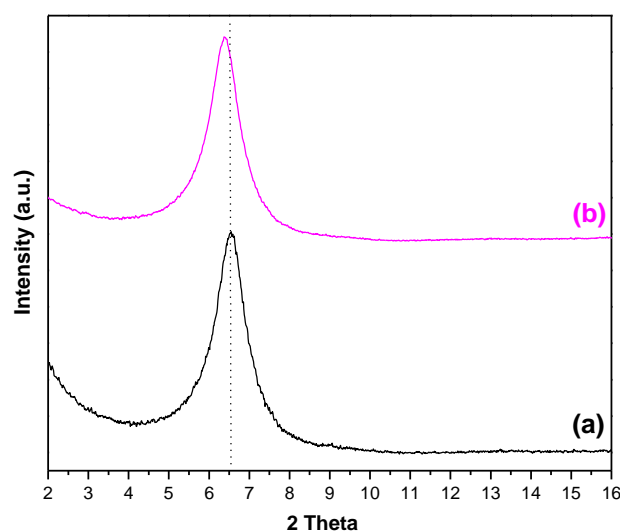


Figure S2. PXRD patterns of GO-DAB₈ sample before (a) and after (b) sequential reaction with *n*-dodecylamine.

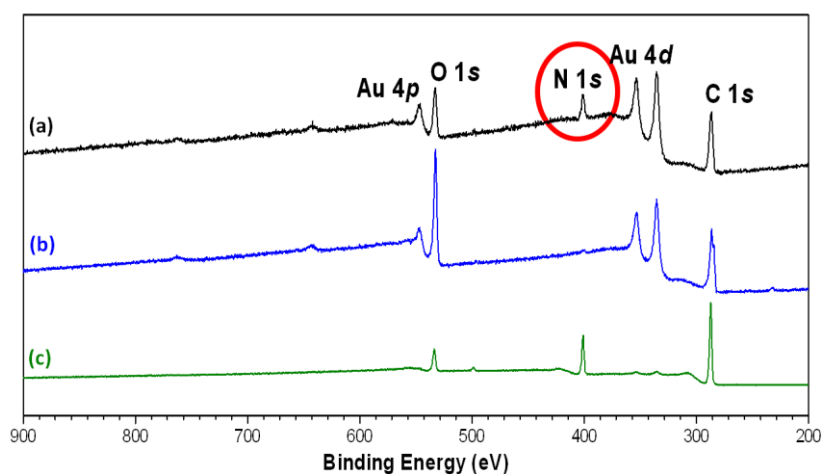


Figure S3. XPS survey spectra of GO-DAB₈ (a). The survey spectra of pristine GO (b) and pure DAB₈ dendrimer (c) are also reported for comparison. The characteristic Au peaks originate from the substrates which were used for the XPS measurements.

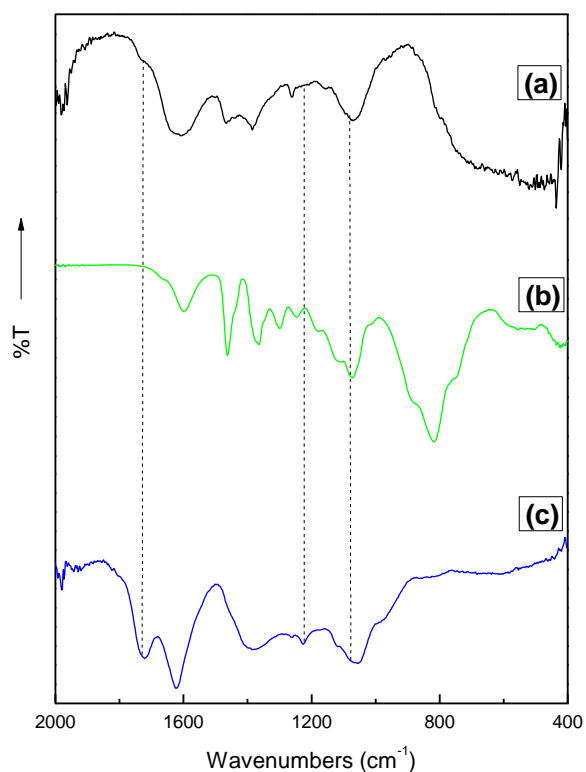


Figure S4. FTIR spectra of GO-DAB₈ (a), pure DAB₈ (b) and pristine GO (c).

For pristine GO, the peaks at 1720 and 1633 cm^{-1} derive from the stretching vibration of carbonyl part of the carboxylic group (C=O) as well as aromatic C=C groups, respectively. The bands at 1387, 1225 and 1062 cm^{-1} originate from carboxy (C-O), epoxy (C-O), and alkoxy (C-O) stretches, respectively. The FTIR spectrum of GO-DAB₈ (Fig. S4a) exhibited major differences; in particular, the stretching band of the epoxy C-O at 1227 cm^{-1} almost disappeared, suggesting the reaction of amino groups of DAB with the epoxy groups of GO via a ring-opening reaction.⁴ Additionally, the intensity of the carboxylic and/or carbonyl C=O stretching band at 1720 cm^{-1} significantly decreased, indicating that amino groups of DAB also interacted with the C=O containing groups of GO. The broad peak of GO-DAB₈ spectrum at $\sim 1070 \text{ cm}^{-1}$ contains overlapping contributions from the C-N stretching vibration of DAB₈ (1110 cm^{-1} , Fig. S4b), the stretching vibration of the alkoxy C-O groups of GO (1062 cm^{-1}) and the newly formed C-N bonds of the intercalated derivative (1039 cm^{-1}). Therefore it is difficult to safely distinguish the band corresponding exclusively to the new C-N bonds.⁵

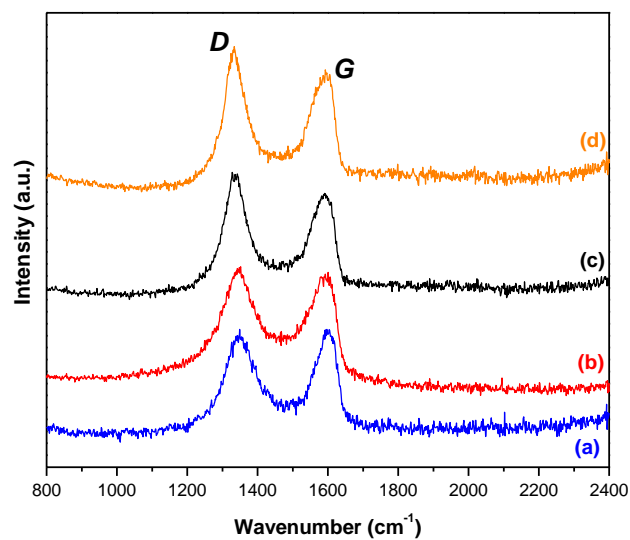


Figure S5. Raman spectra of pristine GO (a) and GO-DAB₄ (b), GO-DAB₈ (c) and GO-DAB₁₆ (d).

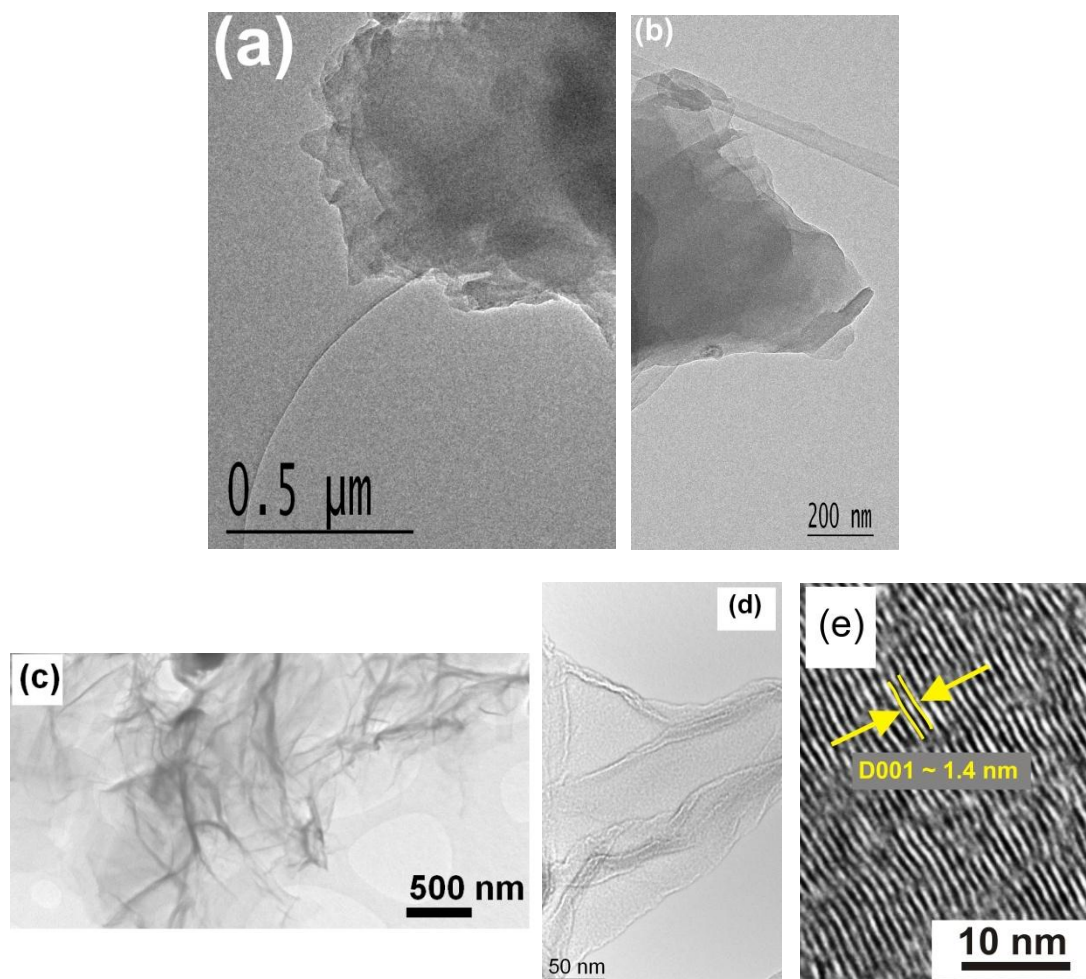


Figure S6. TEM images of pristine GO (a,b) and GO-DAB₈ hybrids (c,d); (e) shows a HR-TEM cross-sectional image of GO-DAB₈ showing the increased inter-sheet distance.

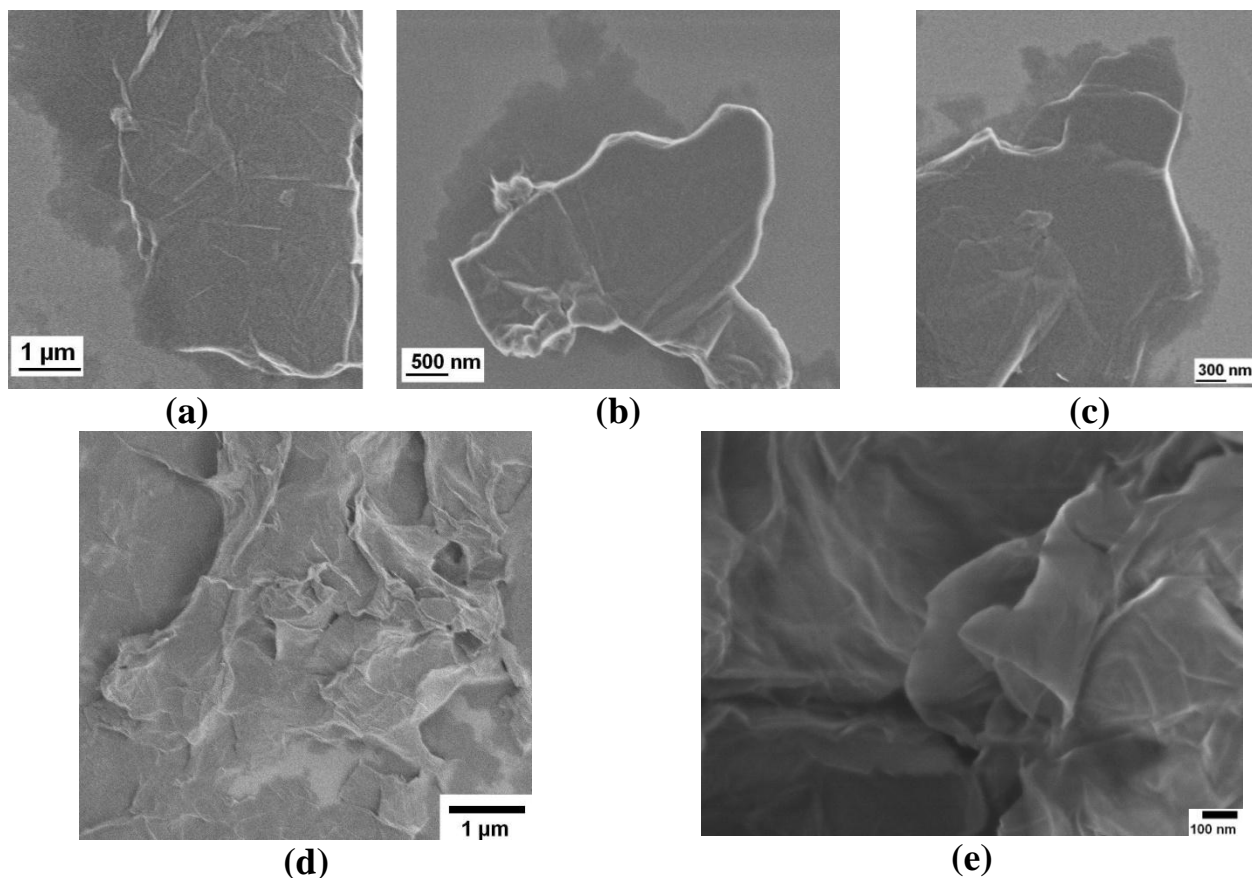


Figure S7. SEM images of pristine GO (a,b,c) and GO-DAB₈ hybrids (d,e).

Table S1: Detailed list of several components along with their mass, material of construction, and density.*

Subscript	Component	Weight (mg)	Material	Density (g/cm ³)	Temperature (K)
s	Dry sample	m_s	GO (reference) or GO-DAB ₈	ρ_s	$T_s = 310.15 \pm 0.01$
s	Wetted sample	-	GO/H ₂ O or intercalated GO/H ₂ O	-	-
1	Wire upper part	42.11	Stainless steel	7.972	$T_c = 303.15 \pm 0.1$
i ₁	Wire lower part	39.45	Stainless steel	-	310.15 ± 0.01
i ₂	Hook	3.64	Stainless steel	-	-
i ₃	Sample pan	267.90	Aluminium	2.643	-
j ₁	Hanging rod	45.02	Stainless steel	7.972	303.15 ± 0.1
j ₂	Pan carrier	47.93	Stainless steel	-	-
j ₃	Counterweight pan	55.20	Aluminium	2.643	-
j ₄	Counterweight	227.10	Pyrex glass	2.230	-

*The density of the dry GO and GO-DAB₈ was obtained as $\rho_s = 0.6 \text{ g/cm}^3$. To investigate absorption kinetics, mass uptake data versus time, were acquired from the sorption microbalance, for each equilibrium pressure and temperature and corrected for buoyancy.

Table S2: CO₂ adsorption capacity of dry and wet GO and GO-DAB₈ samples at a pressure of 1 bar. Included is the H₂O adsorption capacity at several relative pressures.

Sample	H ₂ O adsorption at 310 K	CO ₂ adsorption at 1 bar
	(mmol/g)	298 K / 310 K (mmol/g)
GO reference (<i>dry</i>)	-	1.25 / 1.04
GO reference (<i>wet</i>) P/P ₀ =0.03	2.71	/ 0.49
P/P ₀ =0.13	5.71	/ 0.58
P/P ₀ =0.35	11.2	/ 1.48
GO-DAB ₈ (<i>dry</i>)	-	0.64 / 0.82
GO-DAB ₈ (<i>wet</i>) P/P ₀ = 0.03	1.5	/ 0.63
P/P ₀ =0.13	2.97	/ 0.97
P/P ₀ =0.35	8.16	/ 2.01

At first glance, a comparison between the CO₂ adsorption capacity of the dry GO (reference) and the dry GO-DAB₈ samples (Table S2) could lead to the misleading conclusion that the incorporation of DAB into GO has provoked significant reduction of the empty space available for CO₂ hosting. However there are two significant issues that should be highlighted. Firstly the intercalated sample adsorbs more CO₂ at higher temperature (Table S2). Secondly an intense hysteresis loop is observed solely for the intercalated GO (Fig S8a). Both these observations are related to the sorption mechanism: CO₂ is chemisorbed on grafted amines at low partial pressures while the uptake is primarily achieved by physisorption at high partial pressures.⁶ Additionally, both phenomena reveal constriction effects rather than limited pore space and unveil the significance of adsorption kinetics. Probably in the intercalated GO, the anchored DAB chains are stacked between the GO layers in a quite dense manner, generating very narrow apertures for the passage of CO₂ molecules to the empty space. Indeed, the CO₂ adsorption kinetics for the intercalated sample was much slower compared to the GO (Fig. S8b). As a consequence and despite the prolonged relaxation period applied in each pressure step (more than 18 hours), the CO₂ adsorption in the intercalated GO had not reached equilibrium at any of the examined pressures. However, in humid conditions (real flue gas conditions) the intercalated sample revealed both improved adsorption capacity and faster kinetics.

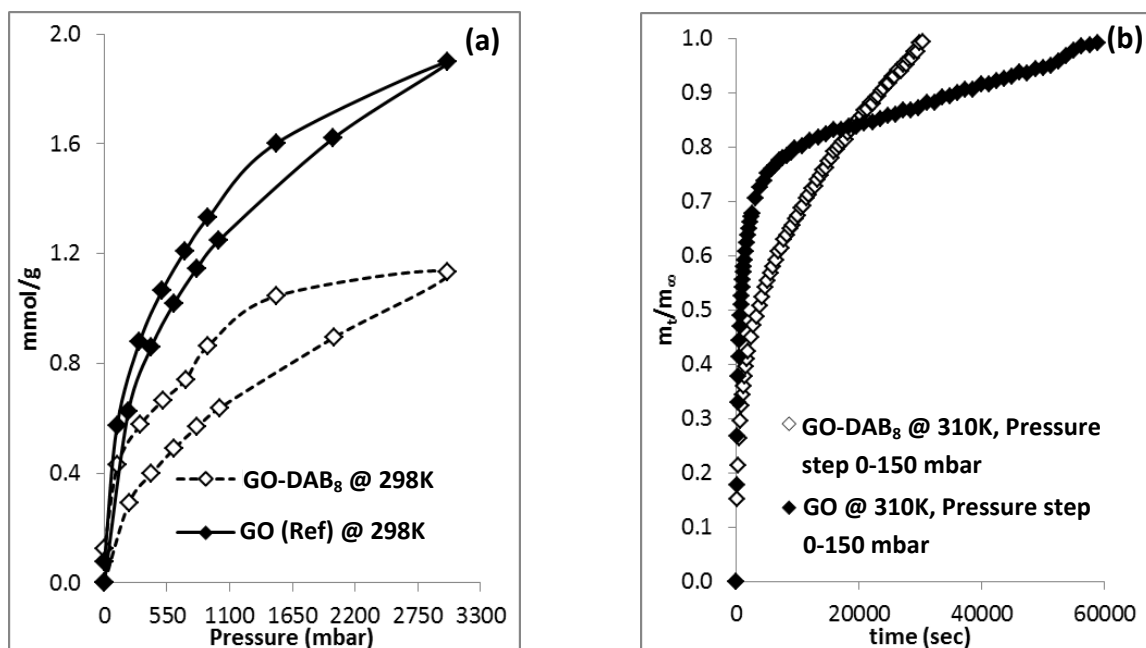


Figure S8: (a) CO₂ adsorption/desorption isotherms of the GO and intercalated GO-DAB₈ samples at 298 K. (b) Kinetics of CO₂ adsorption at 310 K measured with pressure step of 150 mbar.

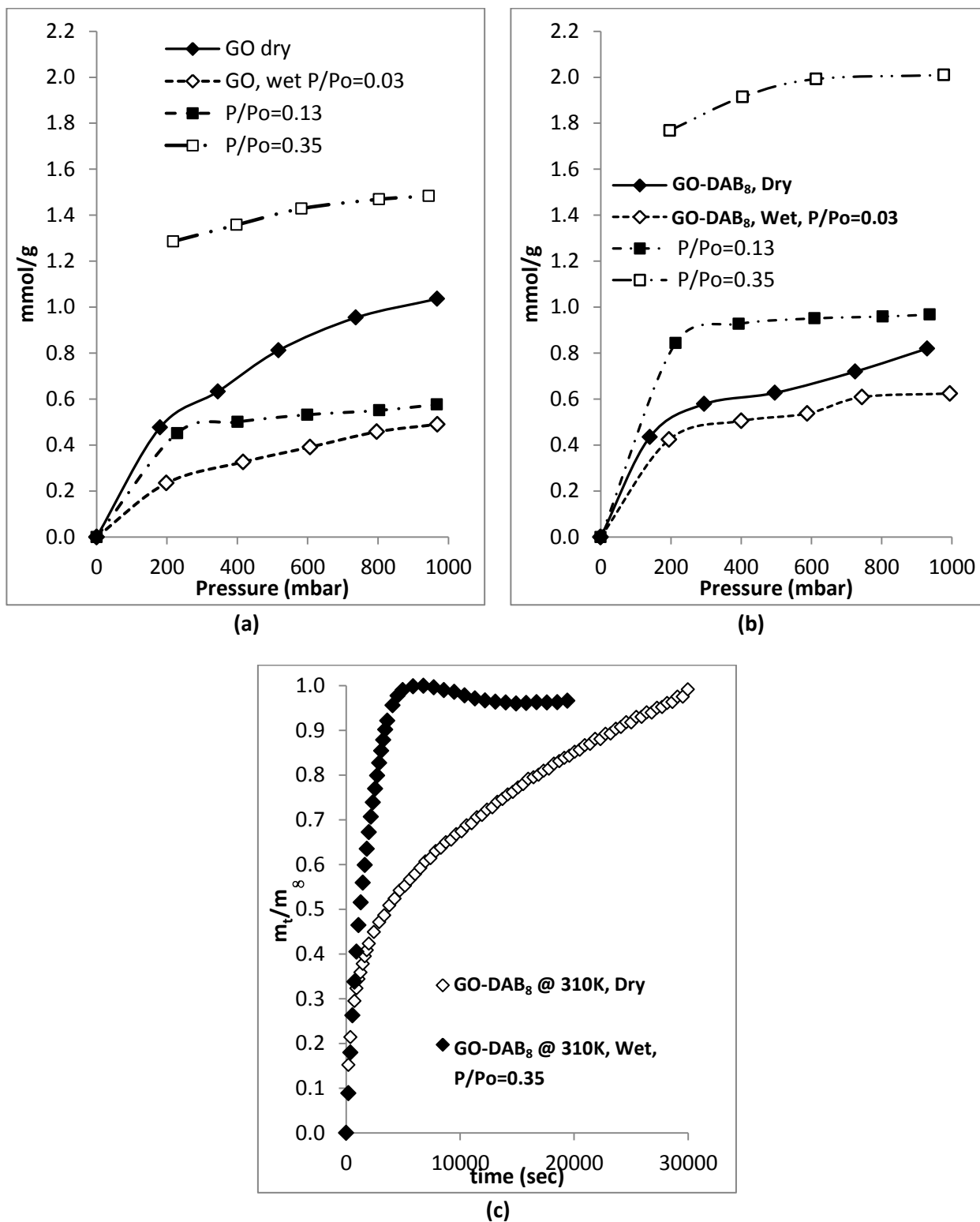


Figure S9: (a) CO₂ adsorption isotherms of the GO at 310 K with the sample equilibrated at several different H₂O vapour relative pressures. (b) Same isotherms for the intercalated GO-DAB₈ sample. (c) Effect of pre-adsorbed water on the CO₂ adsorption kinetics of the intercalated GO-DAB₈ at 310 K measured with a pressure step of 150 mbar.

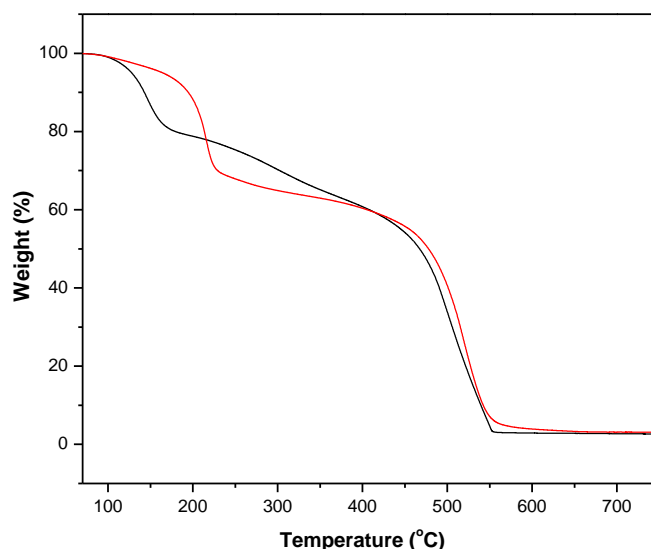


Figure S10: TGA profiles of GO (red) and GO-DAB₈ (1:3 weight ratio, black) measured in air.

For pristine GO, a significant very sharp weight loss corresponding to 29 % of the initial weight was recorded in the temperature range of 170–250 °C, due to the removal of oxygen-containing functional groups present on the graphitic framework. A second significant loss is observed at higher temperatures (>500 °C), and can be attributed to the thermal destruction of the graphitic framework.

On the contrary, the hybrid material exhibits a significant weight loss (~20 %) at around 150 °C. This can be attributed to partial loss or transformation of some GO's oxygen-containing groups either by reaction with amines (ring-opening of epoxides) or by chemical reduction as previously reported in analogous cases of chemically functionalized GO with multi-amine containing molecules.⁷ Therefore TGA measurements provide further experimental evidence that grafting has occurred. The weight loss for GO-DAB₈ in the temperature range 170-250 °C is significantly lower in comparison to GO. This difference in mass loss is attributed to the remaining unreacted GO's oxygen-containing groups, in agreement with previous literature reports of chemically functionalized GO with multi-amine containing species.⁸ The additional weight loss in the temperature range 250-400 °C is assigned to the thermal decomposition of the grafted DAB molecules. Nevertheless, the accurate quantitative calculation cannot be safely performed due to additional weight loss also apparent in the reference material (GO) in the same temperature range. In order to overcome this inconvenience, we performed supplementary elemental analysis measurement towards clarifying the DAB₈ content in the GO-DAB₈ (1:3 weight ratio). Given that the nitrogen signal in the final hybrid originates mainly from DAB₈, the difference compared to the starting GO represents the amount of dendrimer attached at the GO. Therefore, the DAB₈ content in hybrid was calculated from the following formula, DAB₈ (% w/w) = $(N_s - N_{GO}) / (N_{DAB8} - N_{GO}) * 100$, where N_s , N_{DAB8} and N_{GO} , are the nitrogen elemental mass fraction in GO-DAB₈, DAB₈ and GO, respectively (formula previously reported in literature).⁹ The results are summarized in Table S3. According to the elemental analysis results the actual value of DAB₈ weight fraction in GO-DAB₈ hybrid was found 30.7%.

Table S3. Elemental analysis results of GO-DAB₈, DAB₈ and GO

Sample	Sample elemental composition/wt%			DAB ₈ (% w/w)
	C	H	N	
GO	52.93	1.77	0.32	
DAB ₈	61.08	12.94	24.78	
GO-DAB ₈	45.61	5.63	7.82	30.7%

References

- ¹ (a) T. Tsoufis, G. Tuci, S. Caporali, D. Gournis, and G. Giambastiani, *Carbon* 2013, **59**, 100, (b) I. Pavlidis, T. Vorhaben, T. Tsoufis, P. Rudolf, U.T. Bornscheuer, D. Gournis and H. Stamatidis, *Bioresour. Technol.* 2012, **115**, 164.
- ² A. Bourlinos, D. Gournis, D. Petridis, T. Szabó, A. Szeri, and I. Dékány. *Langmuir* 2003, **19**, 6050.
- ³ M. Herrera-Alonso, A.A. Abdala, M.J. McAllister, I.A. Aksay, and R.K. Prud'homme, *Langmuir*, 2007, **23**, 10644.
- ⁴ H. Guo, M. Peng, Z. Zhua and L. Suna, *Nanoscale*, 2013, **5**, 9040.
- ⁵ L.J. Bellamy, *The Infrared Spectra of Complex Molecules*, 3rd Ed. Chapman and Hall, London, 1975.
- ⁶ (a) C. Knofel, C. Matrin, V. Hornebecq, P.L. Llewellyn, *J. Phys. Chem. C* 2009, **113**, 21726; (b) Z. Bacsik, R. Atluri, A.E. Garcia-Bennett, N. Hedin, *Langmuir* 2010, **26**, 10013.
- ⁷ M. Herrera-Alonso *et al*, *Langmuir*, 2007, **23**, 10644.
- ⁸ (a) H. Liu *et al*, *J. Mater. Chem. A*, 2013, **1** 3739; (b) T. Wu *et al*, *J. Mater. Chem.* 2012, **22**, 4722, (c) Z-Y Sui *et al*, *ACS Appl. Mater. & Interfaces*, 2013, **5**, 9172.
- ⁹ X. Zhou, Z. Chen, D. Yan, H. Lu, *J. Mater. Chem.*, 2012, **22** 13506.